J|A|C|S
ARTICLES

Published on Web 01/20/2009

Synthesis of Rod-Shaped Gold Nanorattles with Improved Plasmon Sensitivity and Catalytic Activity

Yuriy Khalavka, Jan Becker, and Carsten Sönnichsen*

Physical Chemistry, Johannes Gutenberg University of Mainz, Jakob Welder Weg 11, Mainz 55128, Germany

Received August 27, 2008; E-mail: soennichsen@uni-mainz.de

Abstract: We prepared rod-shaped gold nanorattles—solid gold nanorods surrounded by a thin gold shell—using a galvanic replacement process starting with silver-coated gold nanorods. These structures are very promising candidates for catalytic applications and optimized plasmon sensors. They combine the advantages of rods (low plasmon resonance frequency, large polarizability, small damping) with the high surface area of hollow structures. The plasmon sensitivity to changes in the dielectric environment is up to 50% higher for gold nanorattles compared to gold nanorods with the same resonance frequency and 6× higher than for plasmons in spherical gold nanoparticles. The catalytic activity measured for the reduction of *p*-nitrophenol is 4× larger than for bare gold nanorods.

Introduction

Since ancient times, the vivid colors of plasmon nanoparticles have been used for decorative purposes.[1] Recently, the extraordinary strong polarizability at the plasmon frequency enables new applications in optical sensing, imaging, and therapy.[2−5] The plasmon frequency depends on the refractive index of the immediate environment,[6] which forms the basis of many sensing schemes.[7] The sensitivity of plasmon sensors for the detection of changes in the environment varies greatly and depends on the particle material and its morphology (shape and size).[8] The first single particle "attoliter" plasmon sensors were realized with spherical gold and silver nanoparticles with relatively low sensitivity.[9−11] The sensitivity has been improved using gold nanoshells,[12,13] rod-shaped[14,15] or bipyramid-shaped nanoparticles.[16] The reason for using nonspherical particles is the desire to shift the plasmon resonance to lower frequencies—away from competing interband transitions—to decrease the plasmon linewidth.[17] Some materials such as silver show smaller plasmon damping than gold but are chemically less stable and more difficult to prepare in the form of nanocrystals with narrow size distribution and without defects. In principle, candidates for very sensitive plasmon sensors have a large part of the plasmon field penetrating the accessible dielectric environment. This favors hollow structures (cages, boxes) or nanoparticle-filled cages (rattles). So far, only a few examples of nanorattles with both core and shell made of metals were reported. Xia and co-workers synthesized spherical nanorattles consisting of Au/Ag alloy cores and shells by means of an electroless galvanic replacement reaction.[18] More recently, a promising synthesis of nanorattles with spherical Au core and Pt/Ag shell has been reported by Yang et al.,[19] but data on their chemical stability and plasmon sensitivity are lacking.

Here, we report a strategy for the preparation of rod-shaped gold nanorattles, i.e. hollow gold nanostructures with a solid nanorod inside (Figure 1). These rod-shaped gold nanorattles combine the advantages of rods (low plasmon resonance frequency, high polarizability, and small plasmon linewidth) with the high surface area of hollow structures and show improved optical sensitivity compared to gold nanorods, spheres, and hollow spheres in the visible range of light. In contrast to the spherical Au/Ag nanorattles reported by Xia et al.,[18] our rod-shaped nanorattles consist entirely of pure gold, making them chemically stable in aqueous environments. Furthermore, we demonstrated that the rattles exhibited higher catalytic

(1) Mulvaney, P. *Langmuir* **1996**, *12*, 788–800.
(2) Eustis, S.; El-Sayed, M. A. *Chem. Soc. Rev.* **2006**, *35*, 209–217.
(3) Daniel, M. C.; Astruc, D. *Chem. Rev.* **2004**, *104*, 293–346.
(4) Perez-Juste, J.; Pastoriza-Santos, I.; Liz-Marzan, L. M.; Mulvaney, P. *Coord. Chem. Rev.* **2005**, *249*, 1870–1901.
(5) Rosi, N. L.; Mirkin, C. A. *Chem. Rev.* **2005**, *105*, 1547–1562.
(6) Murphy, C. J.; Gole, A. M.; Hunyadi, S. E.; Stone, J. W.; Sisco, P. N.; Alkilany, A.; Kinard, B. E.; Hankins, P. *Chem. Commun.* **2008**, 544–557.
(7) Anker, J. N.; Hall, W. P.; Lyandres, O.; Shah, N. C.; Zhao, J.; Van Duyne, R. P. *Nat. Mater.* **2008**, *7*, 442–453.
(8) Lee, K.-S.; El-Sayed, M. A. *J. Phys. Chem. B* **2006**, *110*, 19220–19225.
(9) McFarland, A. D.; Van Duyne, R. P. *Nano Lett.* **2003**, *3*, 1057–1062.
(10) Raschke, G.; Kowarik, S.; Franzl, T.; Sonnichsen, C.; Klar, T. A.; Feldmann, J.; Nichtl, A.; Kurzinger, K. *Nano Lett.* **2003**, *3*, 935–938.
(11) Mock, J. J.; Smith, D. R.; Schultz, S. *Nano Lett.* **2003**, *3*, 485–491.
(12) Sun, Y.; Xia, Y. *Anal. Chem.* **2002**, *74*, 5297–5305.
(13) Raschke, G.; Brogl, S.; Susha, A. S.; Rogach, A. L.; Klar, T. A.; Feldmann, J.; Fieres, B.; Petkov, N.; Bein, T.; Nichtl, A.; Kurzinger, K. *Nano Lett.* **2004**, *4*, 1853–1857.
(14) Nusz, G. J.; Marinakos, S. M.; Curry, A. C.; Dahlin, A.; Hook, F.; Wax, A.; Chilkoti, A. *Anal. Chem.* **2008**, *80*, 984–989.
(15) Baciu, C. L.; Becker, J.; Janshoff, A.; Sönnichsen, C. *Nano Lett.* **2008**, *8*, 1724–1728.
(16) Chen, H.; Kou, X.; Yang, Z.; Ni, W.; Wang, J. *Langmuir* **2008**, *24*, 5233–5237.
(17) Sönnichsen, C.; Franzl, T.; Wilk, T.; von Plessen, G.; Feldmann, J.; Wilson, O.; Mulvaney, P. *Phys. Rev. Lett.* **2002**, *88*, 077402.
(18) Sun, Y.; Wiley, B.; Li, Z.-Y.; Xia, Y. *J. Am. Chem. Soc.* **2004**, *126*, 9399–9406.
(19) Yang, J.; Lu, L.; Wang, H.; Zhang, H. *Scr. Mater.* **2006**, *54*, 159–162.

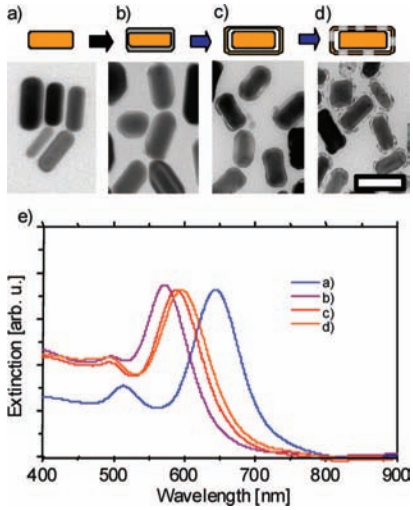

Figure 1. Growth of gold nanorattles. Starting with gold nanorods (a), a silver layer is deposited (b). By means of reaction with Au ions (blue arrows), a shell of Ag−Au grows and then transforms into a cage with the dealloying of silver leading to a closed (c) or porous shell (d), depending on the amount of gold added. Representative TEM images corresponding to all the steps are shown on the bottom (scalebar is 50 nm). Extinction spectra corresponding to each step (e). While the silver coating leads to a blue-shift of the resonance wavelength, the replacement of the silver shell with a gold cage red-shifts the resonance wavelength.

activity compared to gold rods due to the increased surface to volume ratio.

Results and Discussion

Our strategy of rod-shaped nanorattle synthesis closely follows the general procedure used by Xia et al.[18] to form spherical nanorattles with a Au−Ag core. We start with preformed gold nanorods and coat them with a thin silver layer via reduction with ascorbic acid (Asc):

$$2Ag^{+} + H_2Asc + 2OH^{-} \rightarrow 2Ag^{0} + 2H_2O + Asc \qquad (1)$$

In a second step, this silver layer is replaced by gold:

$$3Ag^{0} + [AuC1_4]^{-} \rightarrow Au^{0} + 3Ag^{+} + 4C1^{-} \qquad (2)$$

This leads to the formation of a closed Ag−Au shell (Figure 1c). Further addition of $HAuCl_4$ produces a porous Au cage around the rods (Figure 1d). The silver layer produced by the reduction of silver with ascorbic acid in the presence of poly(vinylpyrrolidone) (PVP) grows epitaxially on the cetyltrimethylamonium bromide (CTAB)-coated gold nanorod surface in contrast to citrate-stabilized spheres.[20,21] We used two thicknesses of silver shells in this study: 3 and 6 nm as estimated from the difference in the mean diameter between coated and bare rods measured on TEM images (Figure S1, Supporting Information). The silver shell leads to the characteristic blue-shift of the plasmon resonance wavelength (Figure S2, Supporting Information).

The second step is a galvanic replacement reaction between the silver shell and an aqueous $HAuCl_4$ solution. Xia et al. performed this step at 100 °C to avoid AgCl coprecipitation during the galvanic replacement reaction.[22] We kept the concentrations of silver and chlorine ions low enough that the solubility product of AgCl is not reached even at room temperature. Since the reaction at room temperature leads to nonuniform cages (Figure S3, Supporting Information), we heated it to 100 °C in order to improve the quality of the outer shell. Hollow rattles form instead of a simple gold shell on a gold core due to the nanoscale Kirkendall effect.[23−26] The higher diffusion rate of silver compared to that of gold and the imbalance of the material flow (see eq 2) leads to an accumulation of vacancies on the inner silver−gold interface.[27] Rattles grown from silver-coated rods with the 6 nm shell are more uniform compared to those grown from the 3 nm shell (Figure S4, Supporting Information). Depending on the amount of gold added in the second step, rattles with closed and porous outer shells were synthesized (Figure 1).

The maximum of the extinction spectra corresponding to the longitudinal plasmon mode of the nanorattles is in-between the maxima for the initial gold nanorods and the silver-coated particles (Figure 1e and Figure S2, Supporting Information). The distance between the shell and the particle is small enough to lead to an effective plasmon coupling, creating a mode similar to that of a completely filled nanoparticle with the same outer dimensions. Since the nanorattles have a lower overall aspect ratio than the initial rods, the resonance wavelength is shifted slightly to the blue compared to the initial rods.

In order to test the plasmon sensitivity to changes in the dielectric environment, we systematically varied the refractive index of the aqueous surrounding by adding sugar, ethylene glycol, or glycerin to suspensions of gold particles. The refractive index n of the solutions was measured with a digital refractometer (Refracto 30PX), and the position of the plasmon resonance peak λ_{res} was determined from its extinction spectrum (Figure S5, Supporting Information). The plasmon resonance shifts linearly to higher wavelength with increasing refractive index n of the surrounding environment (Figure 2a).[6] We used the constant of proportionality ($d\lambda_{res}/dn$) in units of nanometers per refractive index unit (nm/RIU) as a measure for the plasmon sensitivity. In general, the plasmon sensitivity is expected to increase for rods with more red or infrared resonances due to their large polarizability[8]—a trend we observe in these measurements on solid gold nanorods with different resonance wavelength. The sensitivity of gold nanorods is in the range of $d\lambda_{res}/dn = 150-263$ nm/RIU, which is much larger than the values for solid gold spheres ($d\lambda_{res}/dn = 44$ nm/RIU)[16] and gold cubes ($d\lambda_{res}/dn = 83$ nm/RIU)[16] and even larger than the value for spherical hollow gold nanoshells ($d\lambda_{res}/dn = 125$ nm/RIU).[13] Indeed, we observed sensitivity values for rod-shaped gold nanorattles of up to plasmon sensitivity = 285 nm/RIU (Figure 2b), which is also slightly higher compared to recently reported values for gold nanodisks supported on dielectric pillars.[28] The rod-shaped gold nanorattles we produced combine both effects: a shell structure for high surface area and a rod-like shape for efficient light coupling. For some plasmon sensing applications, not the plasmon sensitivity, is important, but the sensitivity in relationship to the plasmon linewidth (fwhm)—the figure of merit (FOM) FOM = plasmon sensitivity/fwhm. The FOM is an important parameter to characterize plasmon sensors if the

(20) Liu, M. Z.; Guyot-Sionnest, P. *J. Phys. Chem. B* **2004**, *108*, 5882–5888.
(21) Becker, J.; Zins, I.; Jakab, A.; Khalavka, Y.; Schubert, O.; Sonnichsen, C. *Nano Lett.* **2008**, *8*, 1719–1723.
(22) Sun, Y.; Xia, Y. *J. Am. Chem. Soc.* **2004**, *126*, 3892–3901.
(23) Kirkendall, E. O. *Trans. AIME* **1942**, *147*, 104–110.
(24) Yin, Y.; Rioux, R. M.; Erdonmez, C. K.; Hughes, S.; Somorjai, G. A.; Alivisatos, A. P. *Science* **2004**, *304*, 711–714.
(25) Fan, H. J.; Gösele, U.; Zacharias, M. *Small* **2007**, *3*, 1660–1671.
(26) Yin, Y.; Erdonmez, C.; and Alivisatos, A. P. Paper LBNL 2006, 60696.
(27) Meyer, R. O. *Phys. Rev.* **1969**, *181*, 1086.
(28) Dmitriev, A.; Hägglund, C.; Chen, S.; Fredriksson, H.; Pakizeh, T.; Käll, M.; Sutherland, D. S. *Nano Lett.* **2008**, *8*, 3893.

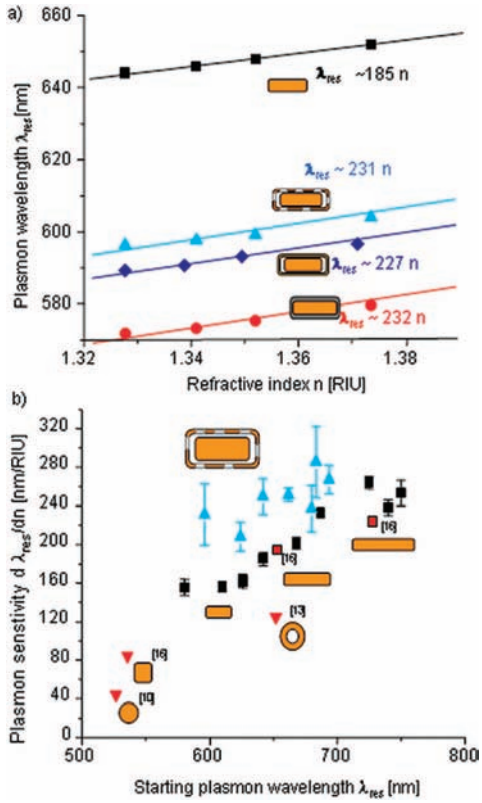

Figure 2. (a) Position of the longitudinal plasmon resonance peak vs refractive index of the surrounding medium for gold nanorods, silver-coated nanorods and nanorattles (as indicated). The slope shows the different sensitivity toward changes in the dielectric environment, and we have indicated the proportionality constants, plasmon sensitivity = $d\lambda_{res}/dn$, for these structures. (b) Overview of the plasmon sensitivity of different gold nanostructures: spheres, cubes, rods, shells, and rod-shaped nanorattles. Since the sensitivity depends not only on shape but also on the position of the resonance wavelength, we show the sensitivity values as a function of the plasmon wavelength in water. The values for spheres, cubes, shells, and some rod samples are taken from the literature (reference numbers as indicated, red labels). Our data for ensemble measurements on different samples of solid gold nanorods (black labels) show lower values for plasmon sensitivity than those of rod-shaped gold nanorattles, produced from these rods (blue labels).

resolution to detect the shifts of plasmon resonance is limited by the resonance linewidth. For the rod-shaped nanorattles, we find the FOM values in the range of 2.1−3.0 compared to 1.2−2.4 for the solid rods used for their synthesis (Figure S6a, Supporting Information). This increase in the FOM for the nanorattles reflects the increase in plasmon sensitivity and almost unchanged plasmon linewidth of the sample after the hollow shell growth.

For practical use of nanorattles in plasmon sensors, the sensitivity in a single particle sensor arrangement is of great importance, where the particles are supported by a substrate, which forms part of a microfluidic flow cell (Figure 3a). The light scattered by single particles is then visualized in a dark-field microscope, where the particles appear as bright-colored spots when illuminated by a white light source (Figure 3b). Single particle spectra are recorded by fast single particle spectroscopy (fastSPS)[29] based on a spatially addressable liquid crystal display used as an entrance to an imaging spectrometer. The fastSPS setup automatically records the spectra of about

(29) Becker, J.; Schubert, O.; Sonnichsen, C. *Nano Lett.* **2007**, *7*, 1664–1669.

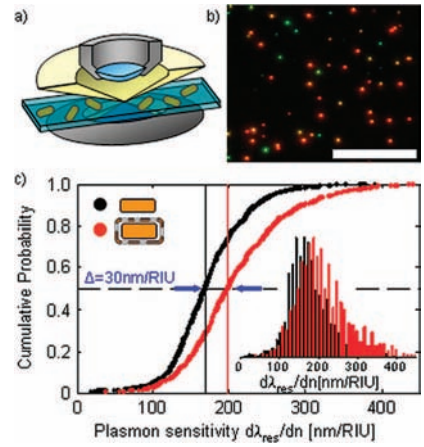

Figure 3. (a) Schematics of the dark-field microscope setup. The illumination passes by the objective, while only the scattered light of the particles is collected and directed to an imaging spectrometer, where the spectrum is captured by a CCD camera. (b) Real color dark-field image of nanorattles, each bright spot represents one single particle (scalebar 25 μm). (c) Cumulative probability distribution of $d\lambda_{res}/dn$ derived from measuring single particle spectra of 1567 nanorods and 803 nanorattles. The median $d\lambda_{res}/dn = 167 \pm 51$ nm/RIU and $d\lambda_{res}/dn = 199 \pm 70$ nm/RIU for the rods (black) and cages (red), respectively. (Inset) Corresponding normalized histograms.

50−100 single particles per measurement, which are initially immersed in distilled water. To measure the nanoparticle's sensitivity toward changes in the dielectric environment, we rinse them with solutions of different refractive indexes [sucrose ($n = 1.378$), ethylene glycol ($n = 1.427$), or dimethylsulfoxide ($n = 1.4785$)] and record the spectra of the previously investigated particles again. In several dozen experiments with different solvents, we investigated a total of 1567 solid gold nanorods and 803 nanorattles. The median plasmon sensitivity of solid gold rods was $[d\lambda_{res}/dn]_{rod} = 169 \pm 51$ nm/RIU and for nanorattles $[d\lambda_{res}/dn]_{rattles} = 199 \pm 70$ nm/RIU (Figure 3c). The relatively large standard deviations in those values is caused both by large interparticle deviations within the same experiment as well as systematic deviations between subsequent experiments with new flow cells, particles, and solvents. Whereas the deviations between particles is expected from the polydispersity of the particles and points toward further chances for improvements, the large deviations in between subsequent experimental runs is puzzling. At present, we have not identified the factor causing these deviations, but we have collected sufficiently high statistics to report precise mean sensitivities (Student's t test proves significantly higher plasmon sensitivity of nanorattles compared to that of solid nanorods with >99.999% probability.). However, previous reports for plasmon sensitivity with fewer statistics have probably overlooked this variation and should be regarded with some caution. Further study of these unexplained variations in plasmon sensitivity, which is independent of the type of particle under investigation, is clearly needed but may require ultraclean working environments. The single particle measurements yielded slightly higher FOM for the solid rods (4.3 ± 1.4) compared to that for the rattles (3.8 ± 1.5) (Figure S6b, Supporting Information) caused by the slightly stronger plasmon damping in rattles which increases the linewidth.

The rod-shaped gold nanorattles we present in this work have two more beneficial properties for applications: chemical stability and enhanced catalytic activity due to their large surface area. The chemical stability against dissolution and oxidation

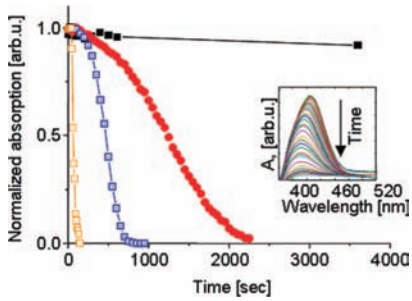

Figure 4. (a) Normalized absorption at the peak position of *p*-nitrophenol as a function of time after the addition of sodium borohydride (black curve). The concentration of *p*-nitrophenol decreases only slowly over time. The presence of metal nanoparticles acting as catalysts significantly increases the reaction rate. The same number of Au-rattles (blue) is more active than nanorods (red). Replacing the outer gold shell in the nanorattles with a thin Pd shell further increases the catalytic activity (orange). The development of the absorption spectra over time is shown in the inset.

in aqueous environment is required for plasmon sensing applications for biological species. Silver-coated gold nanorods, for example, show similar plasmon sensitivity values at visible wavelength (Figure 2a) but are not stable in aqueous environment over time scales of days (Figure S7, Supporting Information). The large surface area of nanorattles, which makes them very sensitive to changes in the dielectric environment, should also enhance their catalytic activity compared to that of solid gold nanorods. To demonstrate this enhanced catalytic activity, we use the reduction of *p*-nitrophenol to *p*-aminophenol by sodium borohydride. It is known that this reaction is catalyzed by metals,[30] and an absorption peak at 420 nm provides an easy way to monitor the reaction spectroscopically. Indeed, we observe a very slow decrease of the nitrophenol absorption for the control experiment without addition of nanoparticles (Figure 4). Adding solid gold nanorods increases the reaction significantly, and all nitrophenol is reduced after about 2000 s. Adding the same number of rod-shaped gold nanorattles further increases the reaction speed by a factor of 3−4. Simple geometrical estimation using average dimension parameters determined from TEM images (Figure S1, Supporting Information) yields a 4 times increase in surface area, which agrees well with kinetic rate increase (Figure S8, Supporting Information). Replacing the $HAuCl_4$ in the cage growth process with $Pd(NO_3)_2$ leads to a Pd shell around the solid gold nanorod (Figure S9, Supporting Information), which increases the reaction speed by another factor of 4 due to the well-known larger catalytic activity of Pd versus Au in this reaction.[31] The shape of the catalytic reduction curve has three regions. At the beginning, the reaction is slow because first sodium borohydride has to be decomposed on the surface of nanoparticles, producing H-atoms, which are then available to *p*-nitrophenol molecules. When the concentration of hydrogen on the surface is maximal, the reaction reaches its highest rate and slows down only when reactants are consumed at the end of the reaction. We find a linear increase of the reaction rate with particle concentration (Figure S10, Supporting Information). The Eley−Rideal mechanism of heterogeneous reactions, which assumes that only one of the reactants (in our case hydrogen) adsorbs on the surface of the catalyst, can explain the observed reaction rate dependencies.

Conclusion

The rod-shaped gold nanorattles or filled nanocages we prepared show beneficial properties when compared to solid gold nanorods: their plasmon resonance shows greater sensitivity to changes in the dielectric environment, and they show larger catalytic activity than solid gold nanorods. Furthermore, these particles are stable in aqueous solution for days, in contrast to silver-coated gold nanorods. They are therefore promising candidates for optimized plasmon binding sensors, detecting changes in the local dielectric environment, and for applications requiring the combination of catalytic activity and plasmon sensing.

Experimental Section

The gold nanoparticles we used here as templates were produced by the seeded-growth technique according to the report by Nikoobath et al.[32] in a highly concentrated aqueous cetyltrimethylammonium bromide solution (CTAB, Sigma-Aldrich).

Silver Coating. We used a procedure described in Liu et al.[20] Solutions of the gold rods are centrifuged once and redispersed in 0.1 M CTAB. 0.8 mL of the CTAB-gold rods solution is diluted in 4 mL of 1 wt % aqueous Polyvinylpyrrolidone (PVP, Aldrich). To the mixture of PVP, CTAB, and gold nanoparticles, we add 180 μL (360 μL) of 1 mM $AgNO_3$ (Sigma-Aldrich) and 100 μL (200 μL) of 0.1 M ascorbic acid (Sigma). Adding 200 μL of 0.1 M NaOH (Merck) starts the coating reaction and leads to a color change within a few minutes. We keep the molar ratio between $AgNO_3$, ascorbic acid, and NaOH constant (0.6:25:50), while the concentration of silver nitrate is changed; 180 μL/360 μL of $AgNO_3$ results in 3 nm/6 nm coating thickness, respectively.

Cage Growth. Silver-coated particles solutions are heated to 100 °C with stirring. Then, either 60 or 120 μL of 1 mM $HAuCl_4$ (Aldrich) is added to rods with 3 nm silver coating, and either 120 or 240 μL of gold solution is added to rods with 6 mm silver coating. In the case of Pd nanorattles, 320 μL of 1 mM $Pd(NO_3)_2$ (Aldrich) is added instead of the gold solution to rods with 6 nm silver coating. The addition of these metal salt solutions is performed dropwise over 10 min with the help of a syringe pump. Afterward, the vial is rapidly cooled in a waterbath.

Ensemble Sensitivity Measurements. Solutions with different refractive indexes are prepared by mixing gold rods, coated particles, or rattles with appropriate volumes of ethylene glycol (EG). After homogenization, optical spectra are recorded with a fiber spectrometer (OceanOptics, USB-2000). The refractive indices of the solutions are measured with a digital refractometer (Refracto 30PX, Mettler Toledo).

Transmission Electron Microscopy (TEM). We use an FEI Tecnai-F30 (300 kV) and Philips CM-12 (120 kV) electron microscopes for TEM imaging.

Single Particle Spectroscopy. The particles are immobilized on a glass substrate by rinsing a diluted solution for 2 min through a flow-cell consisting of a thin, flat glass capillary (0.1 mm × 2 mm × 100 mm) connected to PET tubing. Particles attach randomly to the glass surface. When enough particles are in the field of view, their light scattering spectra are collected by fastSPS.[29]

Catalytic Reduction of *p*-Nitrophenol. Nine milliliters of 3.7×10^{-4} M *p*-nitrophenol (spectrophotometric grade, Sigma) is added to 1 mL of 1.2 M $NaBH_4$ (99%, Aldrich) aqueous solution, and the mixture is stirred for 10 min at room temperature. Aliquots of an aqueous particle suspension (gold nanorods, Au or Pd nanorattles, concentrations approximately 3×10^{10} particles/mL) are added to the mixture. The reaction progress is checked continuously (every

(30) Lee, J.; Park, J. C.; Song, H. *Adv. Mater.* **2008**, *20*, 1523–1528.
(31) Esumi, K.; Isono, R.; Yoshimura, T. *Langmuir* **2004**, *20*, 237–243.
(32) Nikoobakht, B.; El-Sayed, M. A. *Chem. Mater.* **2003**, *15*, 1957–1962.

10 s) by recording optical absorption spectra with a fiber spectrometer (Ocean Optics, USB 4000) until the deep-yellow solution becomes colorless.

Acknowledgment. Inga Zins and Andreas Henkel provided the gold nanorods used in this study. This work was financed in part by the European Union through a NanoSciERA project and by the German Science Foundation (DFG) within the Emmy Noether program. Y.K. and J.B. were supported by MATCOR and Carl Zeiss scholarships, respectively.

Supporting Information Available: Figures showing representative TEM images of silver-coated gold nanorods (S1); optical spectra of gold rods, silver-coated gold rods, and gold nanorattles (S2); TEM images of nanorattles grown at room temperature (S3) and from the thin silver-coated rods (S4); a typical plasmon shift induced by changing the solvents refractive index (S5); figure of merit estimated from bulk and single particle measurements (S6); stability of the particles (S7); the estimation of the surface area of nanorattles (S8); TEM images of Pd-rattles with gold core (S9); and the dependence of the catalytic activity of the gold nanorods and nanorattles on the number of particles added to the reaction mixture (S10). This material is available free of charge via the Internet at http://pubs.acs.org.

JA806766W